

LA-UR-02-0514

Approved for public release;  
distribution is unlimited.

C.1

**Title:** Effects of numerical methods on comparisons between experiments and simulations of shock-accelerated mixing

**Author(s):** William J. Rider, CCS-2; James R. Kamm, CCS-2; Christopher D. Tomkins, P-22; Mark Marr-Lyon, DX-3; Cindy A. Zoldi, X-2; Katherine P. Prestridge, DX-3; Paul M. Rightley, DX-3; Robert F. Benjamin, DX-3

**Submitted to:** Third International Symposium on Finite Volumes for Complex Applications  
24–28 June 2002, Porquerolles, France



## Los Alamos NATIONAL LABORATORY

Los Alamos National Laboratory, an affirmative action/equal opportunity employer, is operated by the University of California for the U.S. Department of Energy under contract W-7405-ENG-36. By acceptance of this article, the publisher recognizes that the U.S. Government retains a nonexclusive, royalty-free license to publish or reproduce the published form of this contribution, or to allow others to do so, for U.S. Government purposes. Los Alamos National Laboratory requests that the publisher identify this article as work performed under the auspices of the U.S. Department of Energy. Los Alamos National Laboratory strongly supports academic freedom and a researcher's right to publish; as an institution, however, the Laboratory does not endorse the viewpoint of a publication or guarantee its technical correctness.

---

# Effects of numerical methods on comparisons between experiments and simulations of shock-accelerated mixing

William Rider\* — James Kamm\* — Chris Tomkins\*\* —  
Cindy Zoldi\*\*\* — Mark Marr-Lyon\*\*\*\* — Kathy Prestridge\*\*\*\*  
— Paul Rightley\*\*\*\* — Robert Benjamin\*\*\*\*

*Los Alamos National Laboratory, CCS-2, MS D413,  
Los Alamos, NM 87545 USA*

*\*Computer and Computational Sciences Division, CCS-2, MS D413,  
wjr@lanl.gov, kammj@lanl.gov*

*\*\*Physics Division, P-22, MS D410,  
ctomkins@lanl.gov*

*\*\*\*Applied Physics Division, X-2, MS B220  
czoldi@lanl.gov*

*\*\*\*\*Dynamic Experimentation Division, DX-3, MS P940,  
mmarr@lanl.gov, kpp@lanl.gov, pright@lanl.gov, rfb@lanl.gov*

---

*ABSTRACT. We consider the detailed structures of mixing flows for Richtmyer-Meshkov experiments of Prestridge et al. [PRE 00] and Tomkins et al. [TOM 01] and examine the most recent measurements from the experimental apparatus. Numerical simulations of these experiments are performed with three different versions of high resolution finite volume Godunov methods. We compare experimental data with simulations for configurations of one and two diffuse cylinders of  $SF_6$  in air using integral measures as well as fractal analysis and continuous wavelet transforms. The details of the initial conditions have a significant effect on the computed results, especially in the case of the double cylinder. Additionally, these comparisons reveal sensitive dependence of the computed solution on the numerical method.*

*KEYWORDS: Richtmyer-Meshkov instability, validation, quantification, multiscale complexity measures.*

---

## 1. Introduction

We examine the detailed structure of experiments and simulations involving shock-driven mixing initiated by the Richtmyer-Meshkov (RM) instability. The experiments consist of a heavy gas ( $\text{SF}_6$ ) that is introduced into a light gas (air) by a nozzle and is impulsively accelerated by a planar Mach 1.2 shock wave; see [RIG 99] for details. In previous work [RID 01], we examined the shock-driven evolution of a varicose-profile, thin gas layer (a gas “curtain”); the present work examines shock interactions with one or two gas cylinders. The fluid mixing in these experiments is driven by the deposition of baroclinic vorticity at the interface between the two fluids, producing the RM instability. Multi-exposure flow visualization is obtained with laser-sheet illumination, providing several snapshots of the  $\text{SF}_6$  volume fraction.

Our computational simulations were performed with different codes and algorithms, to examine the effects of the numerics on the characteristics of the computed mixing flow. The results presented here do not include explicitly modeled viscous terms; complementary simulations of this configuration with equations that *do* contain viscous terms indicate no substantial difference in the computed results. One code we use employs a high resolution Godunov method that is operator split and implemented in a Lagrange-remap (LR) fashion with a linearized two-shock Riemann solver. This code has genuine multimaterial capability, with local thermal, pressure, and momentum equilibrium enforced. This code also has an adaptive mesh refinement (AMR) feature, which was activated in the calculations. The other code is principally used to investigate advanced numerical integration techniques, and uses a Godunov method with a the multimaterial treatment is the same as [BEL 94]. This code employs unsplit differencing (both spatial and temporal) with an adaptive quadratic two-shock Riemann solver [RID 99] in either a standard high-resolution MUSCL-type method or with a new adaptive time integration (ATI) technique.

Experimental images are compared with computed results both qualitatively and quantitatively. Due to the instability driving the flow evolution, statistical methods of comparison are indicated. The quantitative analysis techniques we consider include fractal analysis and continuous wavelet transforms. With these methods we seek to quantify flow structures over a range of length scales. We find that some simulation results correspond quantitatively to experiments, while others deviate significantly. The details of the numerical integration play a strong role in this variation.

## 2. Experiments

Richtmyer-Meshkov experiments were conducted at the Los Alamos facility by Prestridge et al. [PRE 00] and Tomkins et al. [TOM 01]. The experimen-

tal apparatus is a 5.5 m shock tube with a 7.5 cm  $\times$  7.5 cm test section. The driver section is pressurized before the shot, and the rupturing of a polypropylene diaphragm produces a Mach 1.2 planar shock. In the test section, SF<sub>6</sub> gas is injected vertically through a nozzle in the top, and removed through a plenum at the bottom. Interchangeable nozzles with different contours impose perturbations on the cross section of the SF<sub>6</sub>, which has a downward velocity of  $\sim 10$  cm/s. The experiments of interest used single or double column(s) of SF<sub>6</sub>. In the latter case, Tomkins et al. [TOM 01] consider several values of the inter-cylinder spacing  $S$  for fixed cylinder diameter  $D$ ; we examine the three cases  $S/D = 1.2, 1.5,$  and  $2.0$ . The evolving flow, which is imaged by a horizontal laser light sheet, is engineered so that the evolution remains approximately two-dimensional for the span of the experiment. A tracer material consisting of glycol fog (with typical droplet dimension of  $0.5 \mu\text{m}$ ) is added to the SF<sub>6</sub> to greatly enhance the dynamic range of the images, which are captured by CCD camera. The glycol has been shown [RIG 99] to track the SF<sub>6</sub> very accurately. Images, which are obtained at 50, 190, 330, 470, 610, and 750  $\mu\text{s}$  after shock impact with the cylinder(s), have a pixel resolution of  $\sim 0.01 \text{ cm} \times 0.01 \text{ cm}$ . We interpret the image intensity as corresponding to the volume fraction of SF<sub>6</sub>, since the signal registered at the CCD should be proportional to the number of scatterers in each pixel volume times the difference in scattering efficiency between the SF<sub>6</sub>/glycol and air. Table 1 provides the initial gas properties used in the simulations.

### 3. Computations

Several aspects of the numerical simulations greatly influence the computed results. All computations were run in a frame of reference in which the post-shock SF<sub>6</sub> structure is approximately stationary; the translational velocity acts to decrease the horizontal motion of this structure in the computational mesh.

The initial conditions for the SF<sub>6</sub> are critically important because the first shock-cylinder interaction determines much of baroclinic vorticity deposition, which greatly influences the subsequent evolution. Although our previous gas curtain study [RID 01] used experimental data to initialize the simulations, in this work we use idealized initial data. Efforts are underway to obtain high-resolution initial condition images to be used in computational initialization.

Table 1. *Initial gas properties used in the simulations.*

Material	$\rho$ (g cm <sup>-3</sup> )	$p$ (dyn cm <sup>-2</sup> )	$\gamma$	$C_v$ (erg °K g <sup>-1</sup> )	$\eta$ (dyn s cm <sup>-2</sup> )
Pre-Shock Air	$1.00 \times 10^{-3}$	$0.80 \times 10^6$	1.40	$6.89 \times 10^6$	$1.8 \times 10^{-4}$
Post-Shock Air	$1.34 \times 10^{-3}$	$1.21 \times 10^6$	1.40	$6.89 \times 10^6$	$1.8 \times 10^{-4}$
Pre-Shock SF <sub>6</sub>	$5.00 \times 10^{-3}$	$0.80 \times 10^6$	1.09	$5.52 \times 10^6$	$1.5 \times 10^{-4}$

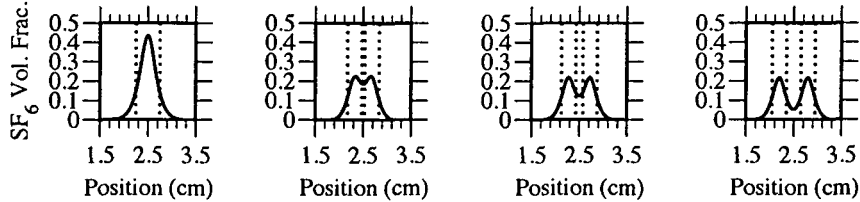


**Figure 1.** Initial volume fractions for the simulations: from left to right, the single cylinder and the  $S/D = 1.2, 1.5,$  and  $2.0$  double cylinders.

For this study, we assign initial conditions by numerically diffusing (with a Laplacian operator) initially uniform circular regions (diameters 0.5 cm and 0.3 cm for the single and double cylinders, respectively) of  $\text{SF}_6$ , using a heuristically chosen number of diffusion iterations so that the initial volume fraction profiles correspond to experimental measurements. Figure 1 contains plots of the  $\text{SF}_6$  volume fraction through each centerline used in each calculation.

Our earlier gas curtain comparisons indicated that the hydrodynamics algorithm plays a significant role in the computed dynamics. Careful consideration of relevant aspects of the basic algorithm, together with numerical tests, suggested that the high-order terms associated with acoustic wave propagation may have affected our earlier gas curtain results. The numerical simulations also exhibited a surprising degree of temporal oscillations; this behavior is also related to sound waves reflecting off the side walls of the shock tube as well as density variations in the flow. Further examination indicated that such features are often not detected by the spatial differencing, which prompted us to consider *temporal* adaptation of the algorithm.

Standard differencing methods are typically adaptive in space, with the time differencing remaining identical for all cells (and usually all time steps). That is, adaptivity—by which we mean differencing algorithm adaptivity, *not* mesh adaptivity—is purely a consequence of the spatial differencing. Instead, we use two independent methods to estimate the time advancement and then nonlinearly merge these results using limiting techniques borrowed from spatial differencing methods. This approach is a *de facto* acknowledgement that the temporal field is varying in a way that is not reflected in the spatial profiles. In a sense, the flow-field is not behaving in a manner consistent with hyperbolic self-similarity, so that time and space differences may not be freely exchanged.

Specifically, we use a linear multistep method (Adams-Bashforth) and a forward-in-time technique (Lax-Wendroff style) to advance the variables. If these results agree to some accuracy, then we choose the smoother of the two values; if they are sufficiently different in magnitude or vary in sign, however, then the time differencing is modified. We note that this modification must

be applied to the fluxes, to insure that the resulting method retains its conservation form. The effect of the temporal adaptation is to make the time differencing a nonlinear—but convex—combination of the two methods based on the smoothness of each time derivative estimate. The results of the temporal limiter are also applied spatially, which appears to ensure stability and provide qualitatively “better” solutions.

#### 4. Results

We focus our analysis on the final experimental volume fraction image, at  $750\mu\text{s}$  after shock-SF<sub>6</sub> contact, to examine the maximum effect of the nonlinear flow evolution. Calculations were run on meshes with  $\Delta x = 0.02, 0.01$  with all schemes and, additionally, at  $\Delta x = 0.005$  for the LR scheme, to a final time of  $750\mu\text{s}$  post-shock. Due to flow instabilities, one cannot expect to compare such images in a pointwise sense, so we evaluate spatial statistical measures at corresponding times. We examine the local fractal dimension ( $D_f$ ) and the continuous wavelet transform (CWT) energy spectrum (see [KAM 01] for details), which provide quantitative measures over a range of length scales.

##### 4.1. Single Cylinder

Results for the single cylinder volume fraction images, local  $D_f$ , and CWT spectra are shown in Figure 2. The local  $D_f$  of the simulations is comparable at small scales, but only the ATI scheme exhibits the increase in  $D_f$  at large scales, which is similar to the experiment; this behavior was also seen in our earlier gas curtain study. All simulations overestimate the CWT energy at smallest scales, but the MUSCL result most closely approximates the experiment over the largest range of scales. Integral scale measures, given in Table 2, show that the ATI scheme most nearly approximates the experimental in these dimensions.

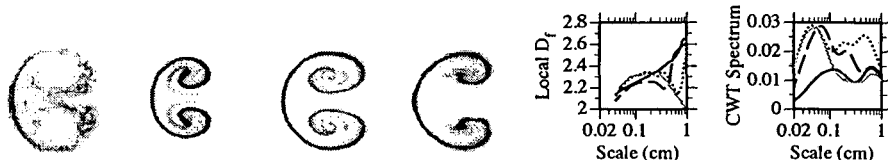


**Figure 2.** From left to right, SF<sub>6</sub> volume fraction images of the single cylinder at  $t = 750\mu\text{s}$  post-shock for the experiment (solid), LR method with  $\Delta x = 0.01\text{ cm}$  (dotted), MUSCL method on the same grid (grey), ATI method on the same grid (dashed), plots of local  $D_f$  and CWT spectrum vs. scale.

Table 2. *Integral scale measures of the cylinders at  $t = 750 \mu s$ .*

Geometry	Height (cm)				Width (cm)				Aspect Ratio			
	Exp.	LR	MUS	ATI	Exp.	LR	MUS	ATI	Exp.	LR	MUS	ATI
Single Cyl.	1.60	1.24	1.30	1.56	1.37	0.93	1.30	1.26	1.17	1.33	1.00	1.23
$S/D = 1.2$	1.28	1.48	1.76	1.69	0.87	0.72	1.01	0.98	1.46	2.06	1.74	1.72
$S/D = 1.5$	1.72	1.64	2.13	1.94	0.76	0.72	0.92	0.95	2.26	2.28	2.32	2.04
$S/D = 2.0$	1.77	1.66	2.30	2.08	0.72	0.69	0.92	1.06	2.45	2.41	2.50	1.96

#### 4.2. Double Cylinder

Results for the volume fraction images, local  $D_f$ , and CWT spectra for these three configurations are shown in Figure 3, 4, and 5, respectively. The  $S/D = 1.2$  configuration shows the tightest coupling of the vortical structures, due to the diffuse initial condition (see Fig. 1); the final state displays structure evocative of the single cylinder case (cf. Fig. 2). The cases with greater initial separation, Figs. 4 and 5, develop two “mushroom caps”, similar to those in idealized RM instability, which rotate under action of the induced vorticity.

In all cases, both LR and ATI methods give less roll-up in the mushroom caps and a more pronounced “bridge” between these structures. For the LR method, this may be related to the minmod limiter used, while the ATI method displays intrinsically greater dissipation. Overall, the gross morphology of the MUSCL result (e.g., the roll-up) appears to approximate the experiment more closely than LR or ATI. The integral scale measures, given in Table 2, are the dimensions of the box that bounds the entire structure; in these measures, the LR results most closely match the experimental data overall.

Examination of the statistical measures does not reveal an unambiguously superior method. In each case, the local  $D_f$  at smaller scales is comparable among the methods; at larger scales, however, the behaviors diverge, with ATI providing greater values, MUSCL giving smaller values, and LR yielding values inbetween. While MUSCL compares best with experiment at intermediate scales, overall LR best reflects the values and behavior of the local  $D_f$  spectrum.

The CWT spectra of the simulations are also comparable at small scales and overshoot the experimental values. At intermediate scales, MUSCL most closely approximates the experiments, while at the largest scales, agreement between simulation and experiment improves, with ATI providing the best results for  $S/D = 1.2$  and  $2.0$ , while MUSCL is superior in the  $S/D = 1.5$  case.

## 5. Summary

We have examined the gas curtain Richtmyer-Meshkov experiments of Prestridge et al. [PRE 00] and Tomkins et al. [TOM 01] together with idealized numerical simulations of these experiments using different hydrodynamics algo-

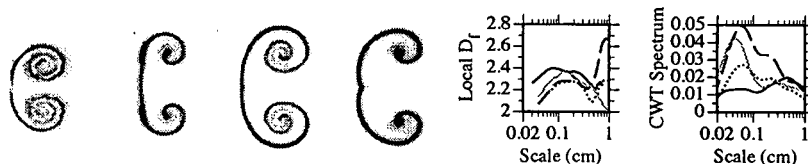


**Figure 3.** From left to right,  $SF_6$  volume fraction images of the  $S/D = 1.2$  double cylinder at  $t = 750\mu s$  post-shock for the experiment (solid), LR with  $\Delta x = 0.01$  cm (dotted), MUSCL on the same grid (grey), ATI on the same grid (dashed), plots of local  $D_f$  and CWT spectrum vs. scale.

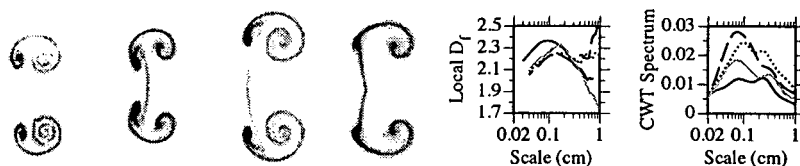


**Figure 4.** From left to right,  $SF_6$  volume fraction images of the  $S/D = 1.5$  double cylinder at  $t = 750\mu s$  post-shock for the experiment (solid), LR with  $\Delta x = 0.01$  cm (dotted), MUSCL on the same grid (grey), ATI on the same grid (dashed), plots of local  $D_f$  and CWT spectrum vs. scale.

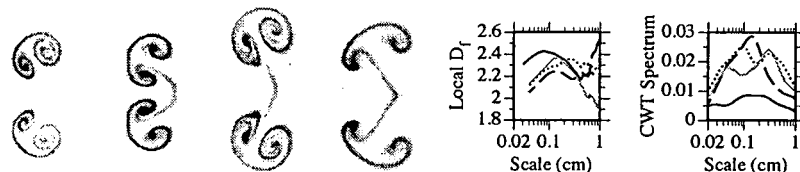


**Figure 5.** From left to right,  $SF_6$  volume fraction images of the  $S/D = 2.0$  double cylinder at  $t = 750\mu s$  post-shock for the experiment (solid), LR with  $\Delta x = 0.01$  cm (dotted), MUSCL on the same grid (grey), ATI on the same grid (dashed), plots of local  $D_f$  and CWT spectrum vs. scale.

rithms. Although the various simulations exhibit qualitatively similar behavior for the single cylinder, for the double cylinder even these gross characteristics vary. Although the new ATI method gave superior results for gas *curtain* simulations initialized with an experimental image, this new adaptive time differencing algorithm does not stand out in the present study of gas *cylinder* simulations using diffused idealized initial conditions. The local fractal dimension spectra are equivocal: for the single cylinder the ATI method appears superior, while for the double cylinder the MUSCL and LR results are arguably better. The wavelet spectra indicate that the MUSCL scheme provides the best overall



results, while the ATI method is comparable at the largest scales. Use of the experimental particle image velocimetry (PIV) capability will help us to better understand the differences between experiments and simulations. Ensembles of experimental and simulation realizations will allow development of bounds on repeatability, and permit quantitative evaluation of mean and fluctuating fields.

#### Acknowledgements

This work is available as Los Alamos National Laboratory report LA-UR-02-\*\*\*\*, and was performed at Los Alamos National Laboratory, which is operated by the University of California for the United States Department of Energy under contract W-7405-ENG-36.

#### References

- [BEL 94] BELL J., BERGER M., SALTZMAN J., WELCOME M., “3-Dimensional Adaptive Mesh Refinement for Hyperbolic Conservation Laws”, *SIAM J. Sci. Comput.*, vol. 15, n°1, 1994, pp. 127–138.
- [KAM 01] KAMM J., RIDER W., RIGHTLEY P., PRESTRIDGE K., BENJAMIN R., P. VOROBIEFF, “The gas curtain experimental technique and analysis methodologies”, *Proceedings of the Tenth International Conference on Computational Methods and Experimental Measurements*, Alicante, Spain 4–6 June 2001, Southampton, WIT Press, 2001, pp. 85–94.
- [PRE 00] PRESTRIDGE K., ZOLDI C., VOROBIEFF P., RIGHTLEY P., BENJAMIN R., “Experiments and simulations of instabilities in a shock-accelerated gas cylinder”, Los Alamos National Laboratory report LA-UR-00-3973, 2000.
- [RID 99] RIDER W., “An Adaptive Riemann Solver Using a Two-Shock Approximation”, *Comp. Fluids*, vol. 28, n°6, 1999, pp. 741–777.
- [RID 01] RIDER W., KAMM J., RIGHTLEY P., PRESTRIDGE K., BENJAMIN R., P. VOROBIEFF, “Direct statistical comparison of hydrodynamic mixing experiments and simulations”, *Proceedings of the Tenth International Conference on Computational Methods and Experimental Measurements*, Alicante, Spain 4–6 June 2001, Southampton, WIT Press, 2001, pp. 199–208.
- [RIG 99] RIGHTLEY P., VOROBIEFF P., MARTIN R., BENJAMIN R., “Experimental Observations of the Mixing Transition in a Shock-accelerated Gas Curtain”, *Phys. Fluids*, vol. 11, n°1, 1999, pp. 186–200.
- [TOM 01] TOMKINS C., PRESTRIDGE K., RIGHTLEY P., VOROBIEFF P., BENJAMIN R., “Flow morphologies of two shock-accelerated, unstable gas cylinders”, *J. Visualization*, to appear, 2002.